Complete analytical description of the working space limits for a manipulator in planar series

Comptes Rendus Mécanique 346 (2018) 13-25
https://doi.org/10.1016/j.crme.2017.10.004

Jérohme Bastien

Laboratoire Interuniversitaire de Biologie de la Motricité
POLYTECH
Université Claude Bernard - Lyon 1
15 Boulevard André LATARJET
69622 Villeurbanne Cedex
France
jerome.bastien@univ-lyon1.fr

summary

We propose a general and analytical method for describing the limits of the planar workspace, i.e. the border of the part of the plan space reached by the end of a human or robot arm. . The proposed method is broken down into three independent steps, none of which calls for calculations of derivatives, determinants or eigenvalues, or using methods of numerical resolution of nonlinear problems, all often used in the literature. The first step, already presented in previous work, consists in geometrically interpreting the necessary degeneration of the Jacobian matrix of the position function, at the edge of the workspace and a condition of alignment of certain joints makes it possible to determine a meeting of arcs of a circle that contain the border. Then, for each of the arcs of a circle, the study of the infinitesimal variation of a point with respect to this circle makes it possible to eliminate all or part of the arcs of a circle previously defined, which is not on the border. Finally, a global course of the meeting of the arcs of circle makes it possible to determine the external border as well as the internal border of the possible hole of the workspace which contains the origin.

Keywords: Robotics; Workspace ; Border; Arms ; Articulation; Biomechanics

1. Presentation of the problem

In robotics as in biomechanics, knowledge of the working space, an area of space that the end of a human limb or the arm of a robot can reach, for example, is fundamental. The border of this workspace must be correctly defined. The joints considered are pivot links, defined by an interval to which the angle between the two segments around the link belongs. In the plane case, this Note is the continuation of works [2,3] where we proposed a local condition necessary but not sufficient for a point in the workspace to be on its border. Founded on a simple geometrical property, this condition made it possible to obtain in analytical form, a set of arcs of circle, without the usual calculations of determinants carried out in symbolism, which contain the border, which constitutes step 0 of the method (see section 2). Having in mind the simplicity and robustness of the proposed method, we now wish to eliminate the parts of the determined arcs of circle which would not be on the border of the workspace. Here again, we propose a general, analytical and complete method, based solely on simple calculations of scalar products, which constitutes step 1 of the method (see section 3). Finally, we propose a global necessary and sufficient condition which makes it possible to analytically give the border in the form of meetings of arcs of a circle (section 4). We will give some possible applications (section 5). Then,

As in [2,3], we consider $\left(O,\vec{i},\vec{j}\right)$ a direct orthonormal reference, p an integer greater than or equal to one, $(l_i)_{1\leq i\leq p}$ p strictly positive numbers, and $\left(\theta_i^+\right)_{1\leq i\leq p}$ and $\left(\theta_i^-\right)_{1\leq i\leq p}$ $2p$ angles with

$$\forall i\in\{1,\dots,p\},\quad -\pi<\theta_i^-<\theta_i^+\leq\pi. \tag{1}$$

We define the workspace as the set of points A_p checking

$$A_0=0,\quad \left(\vec{j},\overrightarrow{0A_1}\right)=\theta_1, \tag{2a}$$

$$\forall i\in\{2,\dots,p\},\quad \left(\overrightarrow{A_{i-2}A_{i-1}},\overrightarrow{A_{i-1}A_i}\right)=\theta_i,\quad \forall i\in\{1,\dots,p\},\quad A_{i-1}A_i=l_i, \tag{2b}$$

and constraints

$$\forall i\in\{1,\dots,p\},\quad \theta_i\in[\theta_i^-,\theta_i^+]. \tag{2c}$$

(see figure 1).

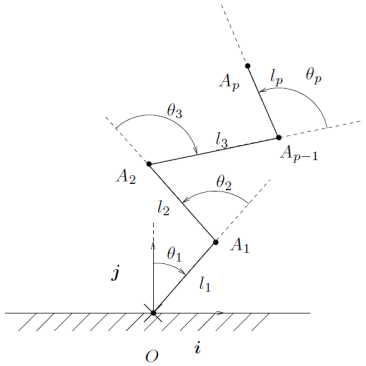

Figure 1. The plan system considered.

We consider the function Φ_p of

$$F=\prod_{i=1}^{p}[\theta_i^-,\theta_i^+], \tag{3}$$

towards $\mathbb{R}^2$, defined by

$$\forall(\theta_1,\dots,\theta_p)\in F,\quad \Phi_p\big(\theta_1,\dots,\theta_p\big)=A_p. \tag{4}$$

Many works naturally relate to the determination of the boundaries of the workspace. For step 0, the function Jacobian $\Phi_p$is necessarily of rank less than one, if the point is on the border. Systematically, this step is resolved symbolically by canceling all the possible extracted determinants [5,6,7,8,9,10]. For step 1, we refer for example to the numerous works of Abdel-Malek [7,11,8]. The calculations presented are valid in a more general framework than ours (2 or 3D, spherical type connections or sliding pivot). The natural condition used is based on a development limited to order 2 locally around a point where the Jacobian is degenerate. The quadratic form associated with the Hessian is studied there. Then the sufficient condition not to be inside the workspace, is programmed in symbolic calculation (with Mathematica ® for example) and the calculation of rank and matrix spectrum are used. These are the signs of the eigenvalues which make it possible to discriminate the different cases.

These calculations are, in theory quite simple, but can have strong numerical instabilities, in addition to being long. On the contrary, we try in this note to use the particular structure of our plan problem. We use in particular the fact that we move locally along a circle. No calculation of derivative or spectrum of matrices is carried out.

Other numerous studies concern the resolution of this problem for manipulators in series or in parallel [12-24]. However, none proposes a general method and these works relate to particular cases (small numbers of degrees of freedom) or are made with numerical approximations or thanks to random simulations.

To our knowledge, only one recent and very interesting work proposes a general method of resolution to determine the limits of the workspace in a very general framework (see [25] and [26, chapter 4 (Workspace Determination)]). But it is a numerical resolution method, based on the method proposed in [27].

2. Stage 0: local condition necessary but not sufficient to belong to the border (reminders).

The border $S=\partial D=D\setminus\mathring{D}$ is traditionally broken down into the form of the following partition $S=S_{\mathrm{I}}\cup S_{\mathrm{II}}\cup S_{\mathrm{III}}\in\mathbb{R}^2$. For S_{I}, all angles θ_i are free (i.e. in $]\theta_i^-,\theta_i^+[$). For S_{II}, there are at least two free components among the p angles (the others being $\theta_i^{\pm}$). For S_{III}, there is only one free component. We have shown in [2,3] that the joints corresponding to configurations of S_{I} and of S_{II} corresponding to free components are necessarily aligned, which made it possible to write and program the complete algorithm of determination of the points verifying this simple geometrical condition. S_{III} is clearly a finite meeting of arcs. We have therefore shown that S is included in a union of arcs of a circle defined by

$$\bigcup_{1\le m\le M}\Phi_p\left(\prod_{k=1}^{p}\Theta_k^m\right), \tag{5}$$

or $\prod$ denotes the Cartesian product and each set $\Theta_k^m$is determined analytically. It is either a singleton or an interval (open or closed). For each m , only one of the setsΘ_k^m is not reduced to a singleton.

Note 1. It is possible that one or more of the parties S_{I}, S_{II} or S_{III} is empty, which does not invalidate the algorithm of step 0, valid for all the values of $\theta_i^{\pm}$.

3. Step 1: sufficient local condition but not necessary so that parts of arcs of a circle are not on the border.

Once we have determined the possible circles to which a point must necessarily belong to be on the border, we look, as is done in a classic way in the literature, the local contribution of the infinitesimal variations of the angles which define this point. If it is possible for this point to evolve on either side of the circle, we deduce that it is not on the border.

On the contrary, if it remains locally on the same side of the circle, we will keep the point or all of these points (that is to say a part of the arc of the circle studied), keeping as information the side in which it is located. This discrimination is usually made through studying symbolism and determining the spectrum and rank of a matrix. On the contrary, in this Note, one can determine in the plane case, the sides where the point studied locally evolves with simple calculations of scalar products.

Let us now study one of the circles defined by (5), corresponding to an integer m fixed and noted $\mathcal{C}_m$. For $i\in\{1,\dots,p\}$, $\Theta_i^m$is an interval not reduced to a singleton. The other intervals are a singleton. The angle θ_i therefore varies in the meantime Θ_i^m. The study of the infinitesimal variation of θ_i brings nothing here, since we know that the point A_p will move along the arc $\mathcal{C}_m$. However, we can assume that each of the anglesθ_j, for $j\neq i$, can vary infinitesimally around its value. For$j\neq i$, consider ε_j defined by

$$\varepsilon_j=\begin{cases}1, & \theta_j=\theta_j^-,\\ -1, & \theta_j=\theta_j^+,\\ 0, & \theta_j\in]\theta_j^-,\theta_j^+[.\end{cases} \tag{6}$$

We define $h={}^t(h_1,\dots,h_p)\in\mathbb{R}^p$ with

$$h_i=0. \tag{7}$$

Consider $\Theta=(\theta_1,\dots,\theta_p)\in\mathbb{R}^p$. Dots$A_k$, for $1\le k\le p$ are dependent on Θ, now fixed and $A_p(\Theta+h)$ designates $\Phi_p(\Theta+h)$. Consider the application $\rho:\mathbb{R}^{p-1}\to\mathbb{R}$, $\tilde{h}=(h_1,\dots,h_{i-1},0,h_{i+1},\dots,h_p)\mapsto\rho\Big(\tilde{h}\Big)$ defined by

$$\rho\Big(\tilde{h}\Big)=A_{i-1}A_p^2(\Theta+\tilde{h})-A_{i-1}A_p^2. \tag{8}$$

By adding null components, corresponding to the component i, we can consider the gradient $B\in\mathcal{M}_{p,1}(\mathbb{R})$ and the hessian (symmetrical) $C\in\mathcal{M}_{p,p}(\mathbb{R})$ of the function ρ, calculated in 0 and write the limited development of ρ to order 2 in the vicinity of $h=0$ Under the form

$$\rho(h)=Bh+{}^thCh+o\Big(\|h\|^2\Big), \tag{9}$$

where h checks (7). Usually (for example in [7]), these elements are computed in symbolic form (formally), given below, in an explicit way.

Lemma 3.1 (Expression of B and diagonal terms of C) *We note σ vector angle rotation $\pi/2$ of $\mathbb{R}^2$. Let's pose $r_j=A_{j-1}A_p$, for $j\in\{1,\dots,p\}\setminus\{i\}$. We have for $j\in\{1,\dots,p\}\setminus\{i\}$:*

$$B_j = 2\overrightarrow{A_{i-1}A_p}.\,\sigma\left(\overrightarrow{A_{j-1}A_p}\right), \tag{10a}$$

$$C_{jj} = r_j^2 - \overrightarrow{A_{i-1}A_p}.\,\overrightarrow{A_{j-1}A_p}. \tag{10b}$$

Lemma 3.2 *We have then, for* $j \in \{1,\dots,p\} \setminus \{i\}$ *:*

- *If j ≤ i-1 , there is* $\alpha \neq 0$ *and* β *dependent only on* $(\theta_k)_{k\in\{j+1,\dots,i-1,i+1,\dots,p\}}$ *with*

$$\sigma\left(\overrightarrow{A_{j-1}A_p}\right).\,\overrightarrow{A_pA_{i-1}} = \alpha\sin(\theta_i+\beta), \quad \forall\theta_i. \tag{11}$$

- *If j ≥ i + 1 , there is* α *dependent only on* $(\theta_k)_{k\in\{i+1,\dots,p\}}$ *with*

$$\sigma\left(\overrightarrow{A_{j-1}A_p}\right).\,\overrightarrow{A_pA_{i-1}} = \alpha, \quad \forall\theta_i. \tag{12}$$

Note 2. The number $\sigma\left(\overrightarrow{A_{j-1}A_p}\right).\,\overrightarrow{A_pA_{i-1}}$ *is of the same sign as the component of the displacement of the point* $A_p(\Theta+h)$ *in the direction of* $\overrightarrow{A_pA_{i-1}}$ *when the angle* h_j *undergoes a positive infinitesimal variation and that all the other components of h are zero.*

We will eliminate the parts of arcs of circle corresponding to points satisfying the following sufficient condition not to be on the border:

$$\forall a \in \mathbb{R}_+^*, \quad \exists h,h' \in \mathbb{R}^p, \Big((7), \Theta+h, \quad \Theta+h' \in F, \quad 0<\|h\|\le a, \quad 0<\|h'\|\le a, \quad \rho(h)\rho(h')<0\Big). \tag{13}$$

Indeed, in this case $A_p(\Theta+h)$ evolves on both sides of the arc $\mathcal{C}_m$.

- At first, unlike the literature, we are content to study only the case where a single component of h is non-zero, the others being zero (local diagonal criterion). So let's fix $j \in \{1,\dots,p\} \setminus \{i\}$. If we note $\rho_j(\kappa) = \rho(0,\dots,0,\kappa,0,\dots 0)$ with $\kappa \in \mathbb{R}$, then (9) is written

$$\rho_j(\kappa) = B_j\kappa + C_{jj}\kappa^2 + o\big(\kappa^2\big), \tag{14}$$

  note that $B_j = 0$ is equivalent to A_{i-1}, A_{j-1} and A_p aligned. According to [2,3], $\varepsilon_j = 0$ therefore implies that $B_j = 0$. We make the reasonable assumption in biomechanics or robotics that the points A_k cannot be confused, which implies that if $B_j = 0$, so $C_{jj} \neq 0$. We therefore have, taking into account (6):

  If $Bj \neq 0$, then $\varepsilon_j \neq 0$ and locally, $\rho_j(\kappa)$ is of the same sign as $B_j\varepsilon_j$ (15a)

  If $Bj = 0$, then $C_{jj} \neq 0$ and locally, $\rho_j(\kappa)$ is of the same sign as C_{jj}. (15b)

  Note that, for this step, knowledge of the alignment of certain points, highlighted geometrically during step 0 (in [2,3]), is therefore fundamental.

  Remark 3. According to remark 2, in the case (15a), one is interested in fact in the normal infinitesimal displacement of a point describing one of the arcs of circle, as also remark Abdel-Malek for example in [7] . Limited development (8) is also present in this work, via the calculation of normal acceleration. In this case (15b), on the other hand, examination of the normal component of the movement alone is no longer sufficient.

  The number B_j depends or not on i, according to Lemmas 3.1 and 3.2. By varying j in $\{1,\dots,p\} \setminus \{i\}$ we can therefore eliminate all the parts of the arcs of circle for which $\rho_j(\kappa)$ changes sign and therefore keep only the parts of arcs of a circle for which the sign of $\rho_j(\kappa)$ is locally constant, i.e.

$$\exists \varepsilon_0 \in \{-1,1\}, \quad \forall j \in \{1,\dots,p\} \setminus \{i\}, \quad \begin{cases} B_j = 0 & \Longrightarrow \varepsilon_0 C_{jj} > 0, \\ B_j \neq 0 & \Longrightarrow \varepsilon_0 \varepsilon_j B_j > 0. \end{cases}$$

- We therefore have, using only the diagonal terms of C, eliminated all the parts of arcs of a circle satisfying a sufficient condition which results in (13). A discussion on the methodology to be adopted from now on and a comparison with the usual methods is presented in Appendix A so as not to burden this text.

Finally, for each of the arcs of (5), either we therefore eliminate all of the studied arc, if none of its points are on the border, or we only keep a part (corresponding to a finite meeting of arcs of a circle). If we make the choice (A.2), it is not certain that the preserved part correspond to points which are locally on the same side of the circle. On the contrary, if we make the choice, (A.7), which takes longer to establish, it is certain that this part corresponds to points which are locally on the same side of the circle and we then know the side of the arc of circle (inside or outside) where the point will evolve locally A_p. Here again we can therefore keep the part of the arcs of a circle which contains only points which surely do not inside it in the form (5).

For all the examples presented here, the choice (A.2) has been made. However, as a check, it is interesting to then set up the choice (A.7) to check a posteriori that all the arcs of the circles kept are guaranteed. It was then noted that all the arcs of circles are guaranteed.

See Figure 6c where the arcs of circle kept from step 1 have been represented, with a small bar for each arc indicating the side where evolves A_p.

4. Step 2: overall condition necessary and sufficient to be on the border.

It now remains to eliminate the parts of an arc defined by (5) which are not on the border, this time using a global criterion. Indeed, locally, the point A_p can remain on the same side of the arc, but the other side of the border can be reached for other angular values far from those which define the arc. Abdel-Malek in [7,8] soberly says that the border of the workspace is the envelope of the previously defined curves.

We start from a point which we are sure belongs to the limit of the workspace: the point furthest from the origin of the set of arcs of circle defined by (5). It is certain that this point belongs to an arc of circle of center the origin. Then, arc of circle by arc of circle, we turn, always in the same direction, by determining, for each intersection of arcs of circle, the one whose direction of the tangent is as close as possible to the arc of circle that we just determined. Then, we keep the portion of this arc between the point considered and the intersection with the nearest arc, among those that remain. The algorithm ends when you return to the starting point. This step is simple in theory: it is indeed each time that we pass from an arc of a circle from the border to the next, to be able to deal with all the cases that may arise: several circles can go through the same point, they can be tangent or concentric. In addition, the calculations being performed numerically, it is necessary to take into account the machine precision in order to predict numerically whether the circles are intersecting, tangent or concentric (see section 6).

The part D being connected but not simply connected, it is possible that its complement is not connected, that is to say that holes appear. The part of the border which we have just defined in the form (5) is the external border, i.e. the common border of $D$and the unbounded component of its complement. To determine the other connected components of the border (the internal borders), our algorithm provides with certainty only the border of the hole containing the origin, if it exists (see figure 6d). In this case, the point closest to the origin is then determined from among the arcs of circle defined by (5). If the hole containing the origin exists,

one is sure again that this point belongs to an arc of circle of center the origin. Then, as before, we determine the arcs of the circle, step by step, stopping when we return to the first point. Here, knowing the possible sides of the interior in relation to the arcs of a circle can be useful for eliminating finished meetings of

We therefore finally completely determined the border of the workspace in the form (5).

5. Applications

Two applications can be proposed immediately using the proposed method (but have not yet been programmed).

First of all, since the border is known as (5), it is possible to solve the opposite problem on the border: that is, a point M of the plane given on the border, we can determine the values of all angles $(\theta_1, \ldots, \theta_p)$ such as $M = \Phi_p(\theta_1, \ldots, \theta_p)$. Let us note, in this respect, that our method makes it possible to propose, for each arc of a circle of the border, a configuration given in (5) making it possible to describe the arc of circle in question. There exist cases where several given configurations make it possible to describe the same portion of arc of circle, thus making the opposite problem with several possible solutions. Consider for example the system with a number of degrees of freedom equal to $p = 2$ and whose values are given by

$$l = (0.30, 0.15)\ (\mathrm{m}),$$
$$\theta^- = (-120, -30)\ (^\circ),$$
$$\theta^+ = (0, 30)\ (^\circ).$$

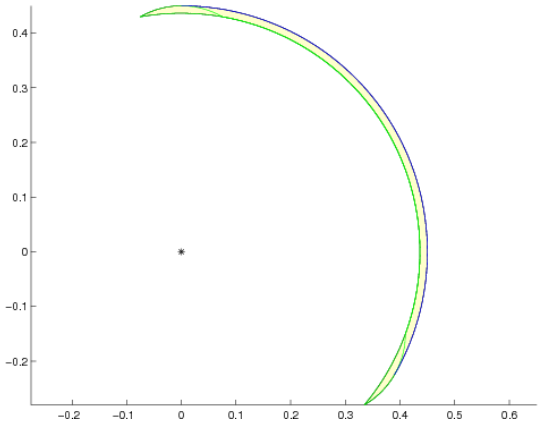

Figure 5. Simulations for $p = 2$. S_{I} is drawn in blue, and $S_{\mathrm{III}}$is drawn in green. The calculated interior of the workspace is drawn in yellow. For step 1, we obtain 7 arcs of a circle.

See figure 5. There are two possible configurations to describe a part of the circle with the origin center and which corresponds to the part of the border closest to the origin.

Another application is a simple criterion to know if a given point on the plane is in the workspace or not. It is clear that thanks to the data of (5), we can know if a point is on the border or not. Suppose it is not on the border. If it is outside the circle of center origin and radius the greatest distance from the origin to the border, it will surely be outside. Finally, by methodically and exhaustively counting the number of points of intersection of a given line segment with a set of circles given by (5) and by considering the parity of the number obtained, we obtain a simple means of knowing if the point is outside or inside a workspace.

6. Implementation

The algorithms used were implemented analytically, but without using symbolic calculation, under Matlab ®. This step therefore used the numerical calculation of Matlab. During steps 0 to 2, it was essentially necessary to determine angles during the transition from Cartesian coordinates to polar coordinates. See details of the algorithm of step 0 in [3]. In addition, during steps 1 and 2, it was necessary to test the nullity or the non-zero sign of certain quantities, which is necessarily done in an approximate manner due to the rounding of calculations. We therefore chose a parameter$\varepsilon > 0$ and replaced for example type equalities $X = 0$ by $|X| \leq \varepsilon$. More precisely, for step 1, we chose $\varepsilon = 1.0\,10^{-12}$ and for step 2, $\varepsilon = 1.0\,10^{-13}$which had to be taken 100 or 1000 times larger in some cases, where p is larger.

In robot design, it is sometimes important to be able to have explicit geometric characteristics of the borders of workspaces. We can therefore use, in this case, the symbolic calculation of Matlab. When passing from Cartesian coordinates to polar coordinates, our codes use Matlab functions `cart2pol` and `atan2`, which do not support symbolic types. However, the functions `acos` and `asin` support them and it would therefore be possible to determine polar coordinates symbolically, insofar as the lengths and angles are themselves converted into symbolic. In this case, one could naturally rigorously test the nullity and the signs of quantities defined in a symbolic way.

7. Numerical simulations

As in [3], for the numerical simulation, we consider a subject of height 1.80 m. The lengths of the upper limb were determined from the anthropometric data of [4]. The lengths of the segments are given as the size ratio (0.108, 0.146 and 0.186 respectively for the hand, forearm and arm for the right upper limb). The angles correspond to the maximum and minimum of the joints, corresponding to the horizontal abduction / adduction of the shoulder (-60 ° / 120 °); flexion / extension of the elbow (0 ° / 130 °) and abduction / adduction of the wrist (-10 ° / 25 °). See Figure 1, where$p = 3$ and O is the shoulder, A_1 the elbow, A_2 the wrist, the segment $0A_1$ is the arm, A_1A_2, forearm and $A_2A_3$the hand. See Table 1 and Figures 2, 3 and 4.

Table 1. Parameters used

case	p	Segment length / size	$(\theta_i^-)_{1 \leq i \leq p}$ ($^\circ$)	$(\theta_i^+)_{1 \leq i \leq p}$ ($^\circ$)	figures
i	1	0.440	-60	120	2
ii	2	0.186; 0.254	-60; 0	120; 130	3
iii	3	0.186; 0.146; 0.108	-60; 0; -10	120; 130; 25	4

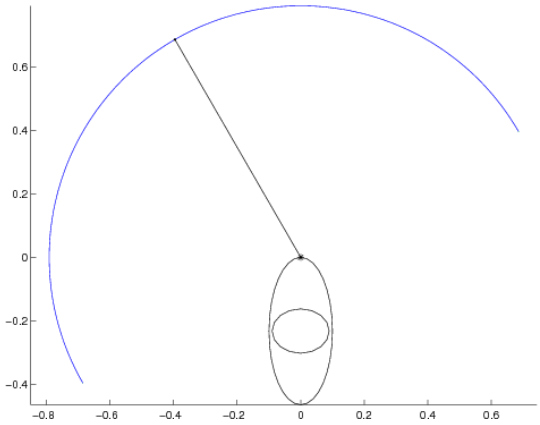

Figure 2. Simulations for $p = 1$. There is only one circular arc (S_{III}) (in blue).

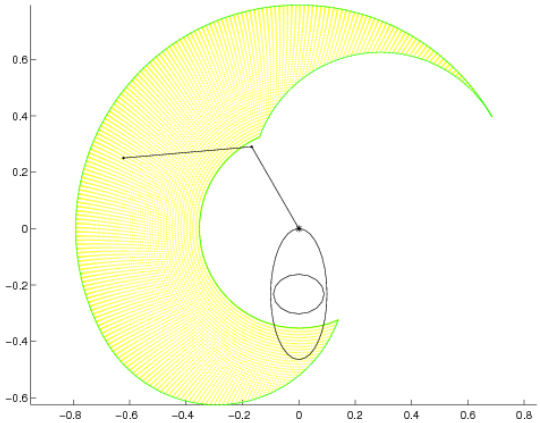

Figure 3. Simulations for $p = 2$. S_{III} is drawn in green. The discrete surface scanned is plotted in yellow. Here, the three steps give the same results. The number of arcs obtained is 4.

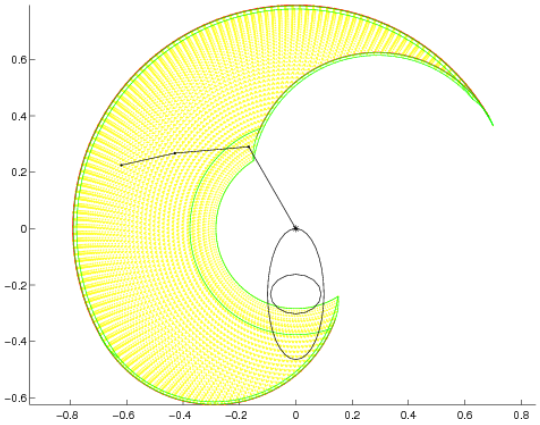

step 0

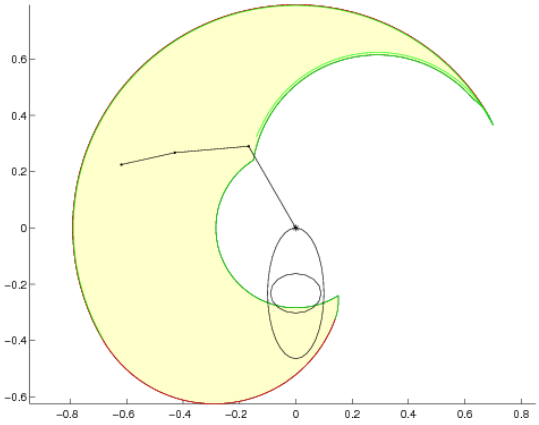

Step 1

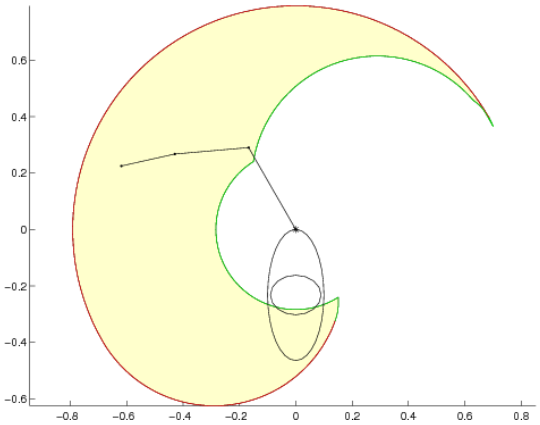

2nd step

Figure 4. Simulations for $p = 3$. S_{II} is drawn in red and S_{III} is drawn in green. The discreet swept area and the calculated interior of the workspace are drawn in yellow. The numbers of arcs corresponding to steps 0,1 and 2 are respectively 16, 11 and 8.

i. Case i corresponds to the free arm, and the forearm and the hand blocked;
ii. Case ii corresponds to the free arm and forearm, hand blocked;
iii. Case iii corresponds to the arm, the forearm and the free hand.

Table 2. Geometric definition of the arcs

of a circle in the form (5).

type	$\Theta_1(^\circ)$	$\Theta_2(^\circ)$	$\Theta_3(^\circ)$
II	$[-60, 120]$	$\{0\}$	$\{0\}$
II	$\{120\}$	$[0, 130]$	$\{0\}$
III	$\{120\}$	$\{130\}$	$[0, 25]$
III	$[-60, 120]$	$\{130\}$	$\{25\}$
III	$\{-60\}$	$[0, 130]$	$\{25\}$
III	$\{-60\}$	$\{0\}$	$[10, 25]$
III	$[-60, -55.1005]$	$\{0\}$	$\{-10\}$
III	$\{-60\}$	$\{0\}$	$[-10, 0]$

We give in Table 2 the description of $S = S_{\mathrm{I}} \cup S_{\mathrm{II}} \cup S_{\mathrm{III}}$ in the form of a union of arcs (5) and the intervals Θ_i for $i \in \{1, 2, 3\}$correspondent, for the full case iii. Each set Θ_i for $i \in \{1, 2, 3\}$is either a singleton or a closed set. All angles in this Note are given in degrees.

Now consider a (virtual) system with a number of degrees of freedom equal to $p = 6$ and whose values are given by

$$
\begin{aligned}
l &= (0.20, 0.20, 0.15, 0.35, 0.20, 0.20),\\
\theta^- &= (-120, -120, -30, -90, -45, -23),\\
\theta^+ &= (60, 170, 30, 91, 23, 24).
\end{aligned}
$$

See figure 6.

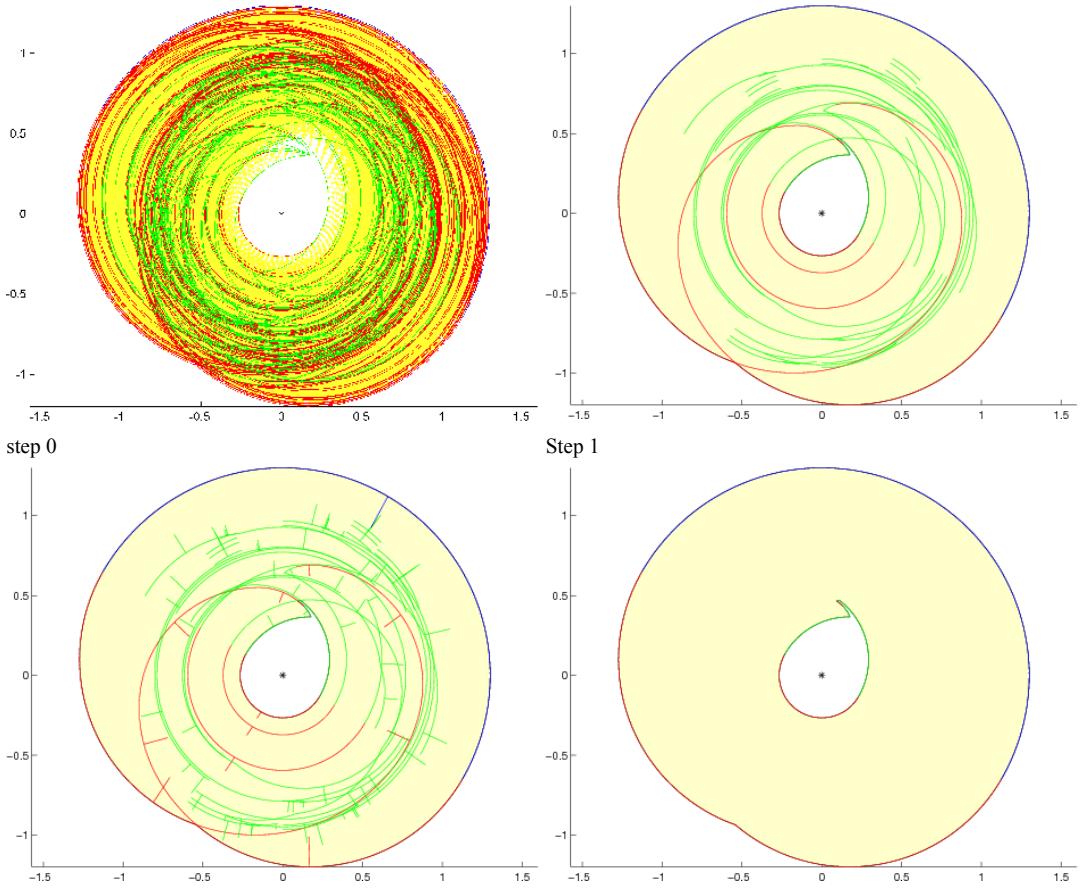

Figure 6. Simulations for $p = 6$. S_{I} is drawn in blue, S_{II} is drawn in red and $S_{\mathrm{III}}$is drawn in green. The discreet swept area and the calculated interior of the workspace are drawn in yellow. The number of arcs corresponding to steps 0,1 and 2 are respectively 506, 75 and 9.

Random prints were made on the corners $\theta^{\pm}$and the lengths l . The number p of segments was varied from 2 to 12 by performing 200 calculations for each value of p . The calculations were made on a computer equipped with Windows 7 Professional, and an Intel (R) Core (TM) i5-6300HQ processor at 2.30 GHz (64 bits)

We had shown in [3], that the algorithm of step 0, the longest, was in $\mathcal{O}(a^p)$ or $a$is real. A linear regression on the decimal logarithm of the computation time confirms this: it gives a correlation equal to 0.9765 and a value of a equal to 3.5289. If we regress the number of arcs in step 0, this also confirms these calculations: it gives a correlation equal to 0.9950 and a value of a equal to 2.7771. For step 1, we find a correlation equal to 0.9356 and a value of a equal to 1.5190. For step 2, the average number of arcs seems to stabilize with p : for $p \geq 5$, we find a number close to 11. We also note that up to $p = 4$, the calculation times are less than 0.1 s and that up $p = 6$, 95% of the calculation times are less than 1.0 s.

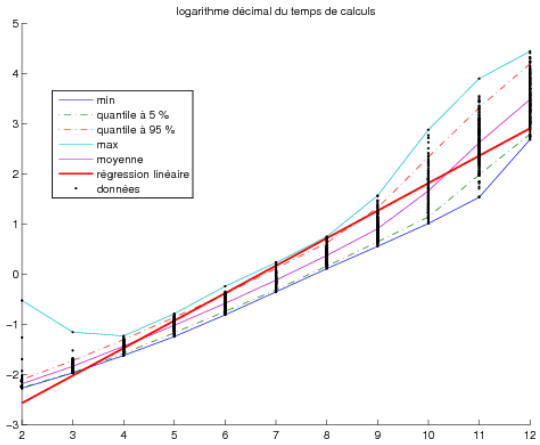

Figure 7. Logarithm of the computation time

See figure 7.

8. Limitations

In practice, according to what is done in the literature, p do not exceed 6, (corresponding to computation times lower than 1.0s). It would seem that until $p = 11$, the calculations are of much longer duration (on average less than 7.0 min.) Beyond, the execution time is enormous (on average greater than 50.9min.). Programmed under Matlab, which is an interpreted language, certain loops (which cannot be parallelized) can be slow. Optimized programming in a compiled language would therefore gain speed.

In Section 4, we discussed the difficulties of detecting internal borders that do not contain the origin. Systematic scanning techniques of graphs would make it possible to detect closed curves which could constitute internal boundaries, by searching for all the possible series of arcs of circles among those detected during step 1.

Finally, the only mathematical constraint respected is the constraint (1). Other constraints may appear for larger values of p than that given in example: it may be that one of the segmentA_iA_{i+1}intersects or is too close to another segment, which is not possible mechanically. We could verify that this case never happens for small values of p . Taking this constraint into account seems to be a much more difficult problem!

9. Conclusion

We have determined the border of a plane workspace in an analytical and explicit way, only by explicit calculations, of angles, of scalar products, of intersections of arcs of circle, without any calculation in symbolism, nor of resolution numeric of nonlinear problems. More intuitive since, based solely on simple calculations of scalar products, this method seems to us more efficient; it does not use symbolic calculation for the calculation of the Jacobian nor the numerical determination of the spectrum of matrix, which is very consumer in computing resources and in computing time.

A natural extension of this work is the extension in dimension 3. More technical, it should be able to extend naturally, by taking again for example the angles of Euler, the rotation matrices and the matrices $(4, 4)$ homogeneous, called Denavit-Hartenberg [28,29] or with the recommendations of [30]. The arcs of a circle would then be replaced by portions of surfaces in space, such as for example spheres or tori. The simple geometrical idea of alignment of step 0 should remain as well as the criterion of step 1. Step 2 would be more subtle, the scanning of the surfaces having to be done in two dimensions.

Annex A. Complements on the method used

We therefore have, using only the diagonal terms of C, eliminated all the parts of arcs of a circle satisfying a sufficient condition which results in (13). However, those that remain do not necessarily verify the negation of (13), which is written:

$$\exists \varepsilon_0 \in \{-1, 1\}, \quad \exists a_0 \in \mathbb{R}_+^*, \quad \forall h \in \mathbb{R}^p, \text{vérifiant } (7)\Big(\Theta + h \in F \text{ et } 0 \leq \|h\| \leq a_0\Big) \Longrightarrow \varepsilon_0 \rho(h) \geq 0. \tag{A.1}$$

In that case $A_p(\Theta + h)$ evolves on the same side of the arc $\mathcal{C}_m$.

- Contrary to the literature, and therefore, more simply, a first choice consists in being satisfied with these calculations: one thus supposes checked the

  diagonal local criterion : defined by (16) where the sign is constant, equal to ε_0. (A.2)

  In this case, (A.1) is only true if h has only a non-zero component. The parts of arcs of a circle which have been preserved therefore have no sign of $\rho(h)$ locally guaranteed. We will see for step 2 (section 4) that we start from a guaranteed arc, that is to say of which we are certain that (A.1) is verified. Gradually, each local sign of $\rho(h)$ will then necessarily be guaranteed. Thus, at the end of the algorithm, for all the parts of arcs of a circle preserved, (A.1) will be true. For this choice, no calculation of rank, spectrum and calculation in symbolism was therefore necessary.
- A second choice now consists in wanting to guarantee the local sign of $\rho(h)$ along the preserved arcs, as is conventionally done. Strictly speaking, this does not bring much, except to eliminate a posteriori some preserved arcs of circle which would not verify (A.1). We will see below, numerically, that these arcs are very few. We then study the quadratic form defined by (9), but which we will determine explicitly and without symbolic calculation as is usually done. In addition, it is only necessary to define the part relating to the angles corresponding to the B_j null, containing the cases where the points are aligned. Indeed, even if it means reordering the elements of$(\varepsilon_j)_{\substack{1 \leq j \leq p \\ j \neq i}}$, B and of C, we can assume without loss of generality, that there is $q \in \{0, \ldots, p-1\}$ with

$$\forall k \in \{1, \ldots, q\}, \quad B_k = 0, \tag{A.3a}$$
$$\forall k \in \{q+1, \ldots, p-1\}, \quad B_k \neq 0. \tag{A.3b}$$

  We then decompose h, B and C in blocks with this partition: $h = \begin{pmatrix} \mathcal{H}_1 \\ \mathcal{H}_2 \end{pmatrix}$, $B = \begin{pmatrix} 0 & \mathcal{B}_2 \end{pmatrix}$, $C = \begin{pmatrix} \mathcal{D} & \mathcal{E} \\ {}^t\mathcal{E} & \mathcal{F} \end{pmatrix}$. We have

$$\rho(h) = {}^t\mathcal{H}_1 \mathcal{D} \mathcal{H}_1 + \varepsilon_0 \sum_{j=q+1}^{p-1} (\varepsilon_0 \varepsilon_j B_j + o(1))|h_j| + o\Big(\|h\|^2\Big).$$

  Taking into account (16) and (A.4), a necessary and sufficient condition for (A.1) to take place is therefore

$$\exists a_0 \in \mathbb{R}_+^*, \quad \forall \mathcal{H}_1 \in \mathbb{R}^q, \text{ vérifiant (6) et (7)}, \quad \big(0 \leq \|\mathcal{H}_1\| \leq a_0 \Longrightarrow \varepsilon_0 {}^t\mathcal{H}_1 \mathcal{D} \mathcal{H}_1 \geq 0\big). \tag{A.5}$$

Conversely, a sufficient (but no longer necessary) condition for (13) to take place is:

$$\exists a_0 \in \mathbb{R}_+^*, \quad \forall \mathcal{H}_1, \mathcal{H}'_1 \in \mathbb{R}^q, \text{ vérifiant (6) et (7) } \big(0 < \|\mathcal{H}_1\| \leq a_0 \text{ et } 0 < \|\mathcal{H}'_1\| \leq a_0\big) \Longrightarrow \big({}^t\mathcal{H}_1 \mathcal{D} \mathcal{H}_1\big)\big({}^t\mathcal{H}'_1 \mathcal{D} \mathcal{H}'_1\big) < 0. \tag{A.6}$$

We are therefore led to make the following second choice, as in the literature:

Total local criterion : defined by (A.5) or (A.6). (A.7)

It is therefore necessary to study the sign of a quadratic form, by classically studying the spectrum of the associated matrix. However, we restrict ourselves to the components corresponding to the aligned points (containing the cases where the corresponding angles are free). We can explicitly determine the coefficients of $\mathcal{D}$, only according to the distances between the points A_k, without going through symbolic calculation, as shown in the following lemma:

Lemma A.1 (Expression of non-diagonal terms of $\mathcal{D}$ (corresponding to the terms B_j null) *For j, j' in $\{1, \ldots, q\}$ with $j \leq j'$, dots A_{i-1}, A_{j-1}, $A_{j'-1}$ and A_p are aligned and we have*

$$\mathcal{D}_{jj'} = \overline{A_{j-1}A_p}\,\overline{A_{j'-1}A_p} - \overline{A_{i-1}A_p}\,\overline{A_{j'-1}A_p}.$$

There are simple sufficient conditions, not expressed here, relating to $\mathcal{D}$, without going through its spectrum, which ensure that (A.5) or (A.6) is verified. In this case, all the arcs of circles have a guaranteed sign. As a last resort, if none of them is verified, then as in the literature, the spectrum of $\mathcal{D}$. We will see, numerically, that these cases are very rare

References

1. J.F.M. Molenbroek. Reach envelopes of older adults.
   In : The 42-nd Annual Meeting of the "Human Factors and Ergonomics Society", pages 166-170, Chicago, USA, 1998.
2. Jérohme Bastien, Pierre Legreneur, and Karine Monteil.
   Caractérisation géométrique de la frontière de l'espace de travail d'un système polyarticulé dans le plan.
   Comptes Rendus de l'Académie des Sciences (Mécanique), 335 (3): 181-186, 2007.
3. Jérohme Bastien, Pierre Legreneur, and Karine Monteil.
   A geometrical alternative to jacobian rank deficiency method for planar workspace characterisation. Mechanism and Machine Theory, 45: 335-348, 2010.
4. D.A. Winter. Biomechanics and Motor Control of Human Movement. John Wiley & Sons, New Jersey, Canada, 4 edition, 2009.
5. Karim Abdel-Malek, Frederick Adkins, Harn-You Yeh, and Edward Haug. On the determination of boundaries to manipulator workspaces.
   Robotic and Computer Integrated Manufacturing, 13 (1): 63-72, 1997.
6. Karim Abdel-Malek and Harn-You Yeh. Geometric representation of the swept volum using jacobain rank-deficiency conditions.
   Computer Aided Design, 29(6):457-468, 1997.
7. Karim Abdel-Malek, Harn-You Yeh, and Othman Saeb. Swept volumes: void and boundary identification.
   Computer-Aided Design, 30(13):1009-1018, 1998.
8. Karim Abdel-Malek, Jingzhou Yang, Richard Brand, and Emad Tanbour. Towards understanding the workspace of human limbs.
   Ergonomics, 47(13):1386-1405, 2004.
9. E.Dupuis, E.Papadopoulos, and V.Hayward.
   The Singular Vector Algorithm for the Computation of Rank- Deficiency Loci of Rectangular Jacobians.
   In : International Conference on Intelligent Robots and Systems, Maui, Hawai, USA, 2001.
10. Jingzhou Yang, Yunqing Zhang, Liping Chen, and Karim Abdel-Malek. Reach envelope of human extremities.
    Tsinghua Sci. Technol., 9(6):653-666, 2004.
11. Karim Abdel-Malek, Harn-Jou Yeh, and Saib Othman. Interior and exterior boundaries to the workspace of mechanical manipulators.
    Robotics and Computer Integrated Manufacturing, 16:365-376, 2000.
12. Mazen Zein, Philippe Wenger, and Damien Chablat.
    An exhaustive study of the workspace topologies of all 3R orthogonal manipulators with geometric simplifications.
    Mech. Mach. Theory, 41(8):971-986, 2006.
13. A.M. Hay and J.A. Snyman. The determination of nonconvex workspaces of generally constrained planar Stewart platforms.
    Comput. Math. Appl., 40(8-9):1043-1060, 2000.
14. Andrzej J. Cebula and Paul J. Zsombor-Murray. Formulation of the workspace equation for wrist-partitioned spatial manipulators.
    Mechanism and Machine Theory, 41(7):778-789, 2006.
15. Sen Dibakar and T.S. Mruthyunjaya.
    A computational geometry approach for determination of boundary of workspaces of planar manipulators with arbitrary topology.
    Mechanism and Machine Theory, 34:149-169, 1999.
16. Jean-Pierre Merlet, Clément M. Gosselin, and Nicolas Mouly. Workspaces of planar parallel manipulators.
    Mech. Mach. Theory, 33(1-2):7-20, 1998.
17. M. Husty, E. Ottaviano, and M. Ceccarelli. A geometrical characterization of workspace singularities in 3R manipulators.
    In : Advances in robot kinematics: analysis and design, pages 411-418. Springer, New York, 2008.
18. Nives Klopcar and Jadran Lenarcic. Kinematic model for determination of human arm reachable workspace. Meccanica, 40(2):203-219, 2005.
19. Xin-Jun Liu, Jinsong Wang, and G. Pritschow. Kinematics, singularity and workspace of planar 5R symmetrical parallel mechanisms.
    Mechanism and Machine Theory, 41(2):145-169, 2006.
20. Haidong Li, Cl\'ement M. Gosselin, and Marc J. Richard.
    Determination of maximal singularity-free zones in the workspace of planar three-degree-of-freedom parallel mechanisms.
    Mech. Mach. Theory, 41(10):1157-1167, 2006.
21. Jing-Shan Zhao, Min Chen, Kai Zhou, Jing-Xin Dong, and Zhi-Jing Feng.
    Workspace of parallel manipulators with symmetric identical kinematic chains. Mech. Mach. Theory, 41(6):632-645, 2006.
22. P. Jauer, I. Kuhlemann, F. Ernst, and A. Schweikard. Gpu-based real-time 3d workspace generation of arbitrary serial manipulators.
    In : The 2nd International Conference on Control, Automation and Robotics (ICCAR), 2016.
23. Ilian A. Bonev and Clément M. Gosselin. Analytical determination of the workspace of symmetrical spherical parallel mechanisms.
    IEEE Transactions on Robotics, 22(5):1011-1017, 2006.
24. Marc Arsenault and Clément M. Gosselin. Kinematic, static and dynamic analysis of a planar 2-DOF tensegrity mechanism.
    Mech. Mach. Theory, 41(9):1072-1089, 2006.
25. Oriol Bohigas, Montserrat Manubens, and Lluis Ros.
    A complete method for workspace boundary determination on general structure manipulators.
    IEEE Transactions on Robotics, 28(5):993-1006, 2012.

26. Oriol Bohigas, Montserrat Manubens, and Lluis Ros. Singularities of robot mechanisms, volume 41 of Mechanisms and Machine Science. Springer, Cham, 2017. Numerical computation and avoidance path planning.
27. Josep M. Porta, Lluis Ros, and Federico Thomas. A linear relaxation technique for the position analysis of multiloop linkages. IEEE Transactions on Robotics, 25(2):225-239, 2009.
28. J. Denavit and R. S. Hartenberg. A kinematic notation for lower-pair mechanisms based on matrices. J. Appl. Mech., 22:215-221, 1955.
29. Giovanni Legnani, Federico Casolo, Paolo Righettini, and Bruno Zappa. A homogeneous matrix approach to 3d kinematics and dynamics - i. theory. Mechanism and Machine Theory, 31(5):573-587, 1996.
30. G. Wu, F.C.T van der Helm, M. Veeger, H.E.J. Makhsous, P. Van Roy, C. Anglin, J. Nagels, A.R. Karduna, K. McQuade, X. Wang, and al. Isb recommendation on definitions of joint coordinate systems of various joints for the reporting of human joint motion-part ii: shoulder, elbow, wı Journal of Biomechanics, 38(5):981-992, 2005.